Transactions in GIS, 2004, 8(2): 191–209

Research Article

Development and Application of 2D and 3D GRASS Modules for Simulation of Thermally Driven Slope Winds

Marco Ciolli
Dipartimento di Ingegneria Civile e Ambientale
Università degli Studi di Trento

Massimiliano de Franceschi
Dipartimento di Ingegneria Civile e Ambientale
Università degli Studi di Trento

Roberto Rea
Dipartimento di Ingegneria Civile e Ambientale
Università degli Studi di Trento

Alfonso Vitti
Dipartimento di Ingegneria Civile e Ambientale
Università degli Studi di Trento

Dino Zardi
Dipartimento di Ingegneria Civile e Ambientale
Università degli Studi di Trento

Paolo Zatelli
Dipartimento di Ingegneria Civile e Ambientale
Università degli Studi di Trento

Abstract
The ability to manage and process fully three-dimensional information has only recently been made available for a few Geographical Information Systems (GIS). An example of integrated and complementary use of 2D and 3D GRASS modules for the evaluation and representation of thermally induced slope winds over complex terrain is presented. The analytic solution provided by Prandtl (1942) to evaluate wind velocity and (potential) temperature anomaly induced by either diurnal heating or nocturnal cooling on a constant angle slope is adopted to evaluate wind and temperature profiles at any point over both idealised and real complex terrain. As these quantities depend on the slope angle of the ground and on the distance from the slope surface suitable procedures are introduced to determine the coordinate n of a point in the 3D volume measured along the direction locally normal to the terrain surface. A new GRASS module has been developed to evaluate this quantity and to generate a 3D raster file where each cell is assigned the value of the cell on the surface belonging to the normal vector. The application of the algorithm implemented in

Address for correspondence: Dipartimento di Ingegneria Civile e Ambientale, Università degli Studi di Trento, Via Mesiano 77 – 38100 Trento, Italy. E-mail: marco.ciolli@ing.unitn.it

GRASS to an ideal valley and to a real valley close to the city of Trento in the Alps provides results in accordance with data reported in the literature. An extension of Prandtl's (1942) model to take into account humidity and evaporation processes on the soil is also proposed and implemented.

1 Introduction

The convergence of mathematical models investigating spatial phenomena and GIS has been difficult because of the high specialization of the models and of their authors on the one hand, and of the lack of real 3D support from GIS on the other hand. However, the integration of these two tools leads to great advantages both for the model implementation and for the availability of the results. The model implementation benefits from an integrated environment for the management of spatial and semantic data, with routines for numerical and cartographic I/O (Input/Output). The results of the model application in a GIS reach a broader audience and can be integrated into a wide range of environmental analysis.

The recent availability of a full 3D implementation in GRASS (Neteler and Mitasova 2002) has been exploited to set up two different models to depict the behaviour of the thermally driven winds over a tilted slope. The distribution of other atmospheric variables strictly tied to wind velocity, such as air temperature and humidity, is also evaluated.

The availability of GRASS GIS under GNU Public Licence (GPL) has made possible the direct access to its source code, therefore the possibility of developing a new module solving the problem of evaluating the distance of a point in the (3D) space from a surface, represented by a digital terrain model (DTM) along the normal direction. Moreover, this new module can be used to "transport" values from the surface to the 3D domain, where they are used to evaluate the atmospheric variables.

2 Coupling GIS and Atmospheric Models

The coupling of GIS and atmospheric models brings significant advantages but some requirements must be taken into account.

The advantages of this integration have been briefly outlined in the previous section; both atmospheric scientists and GIS users benefit from this. Section 4 will show how the model implementation can be made easy by the availability of 2D and 3D data structures and management functions in a GIS. On the other hand, the possibility of the evaluation of atmospheric quantities (wind speed, air temperature and humidity) at the local scale can improve environmental analysis in a significant way.

The requirements are mainly related to the availability of a real 3D data structure and a suitable management system. The most specific issue, with respect to the usual GIS use, that arises when coupling GIS and atmospheric models is the mixing of 2D and 3D data. In fact, while the latter constitute the model representation of the problem domain and therefore the solution domain, 2D data represent the boundary conditions for the model. These boundary conditions data (soil features, coverage and so on) are data usually already available in a GIS environment, where they can be easily managed. However, some quantities needed by the atmospheric model are not usually available, not even when a full 3D support is present. The most notable example is the possibility

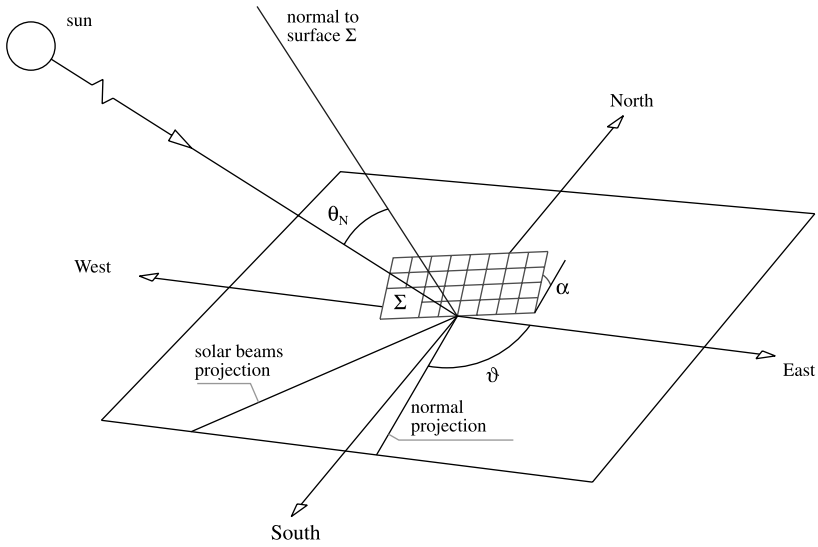

Figure 1 Solar irradiance on a tilted surface

of evaluating the distance of a point in the 3D space from the terrain surface along the normal direction. Section 4 shows two possible solutions of this problem in GRASS.

For the evaluation of the effectiveness of the model implementation a tool for the exploration of the results, represented by the 3D values of atmospheric quantities, must be available. The good integration of many Open Source software projects has made easy the use of VIS5D+ (http://vis5d.sourceforge.net/), a system for interactive visualization of large 5-D gridded data sets.

3 Solar Radiation and Slope Winds

The intensity S of solar radiation per unit surface normal to sun beams at the outermost atmospheric layers is referred to as *extraterrestrial solar irradiance* or the *solar constant*. Its value ranges between 1,360 and 1,380 W m^{-2}. Solar irradiance at ground level is a fraction of the extraterrestrial solar irradiance, after reflection and absorption by various atmospheric components, like water vapour, clouds and aerosols. It also depends on the angle between the normal to the terrain surface and the sun beam as outlined in Figure 1. This implies a strong dependence on season, daytime hour and local orientation of the ground surface.

Solar irradiance at the ground surface is partly reflected back by the terrain, while the remaining amount is converted partly in heat flux into the ground and partly in either sensible or latent heat flux imparted to the adjacent air layers. The budget of the above components can be simply stated as:

$$-Q_s^* = Q_H + Q_E - Q_G \tag{1}$$

where Q_s^* is the net radiation flux, Q_H is the sensible heat flux, Q_E is the latent heat flux and Q_G ground heat flux (fluxes from ground to the atmosphere are positive). A sketch of the above budget is outlined in Figure 2.

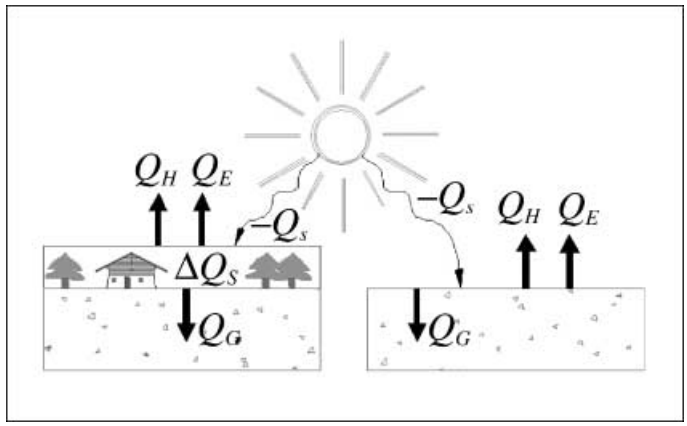

Figure 2 Heat fluxes for a thin air layer during day time

During daytime $-Q_s^*$ is positive, sensible heat flux Q_H and latent heat flux Q_E are positive due to thermal conduction and humidity transport phenomena, respectively. Heat flux into the ground $-Q_G$ is positive, being the energy transferred from the heated surface to the cooler terrain. During nighttime $-Q_s^*$ is often negative, due to the long-wave radiation (IR) emitted toward the atmosphere, Q_H is negative and Q_E is negative due to dew or frost formation. In dry conditions Q_E is very small and can be neglected. The heat flux from the warm soil layers to the colder surface $-Q_G$ is negative too.

In meteorological applications, as well as in the present case, sensible heat flux imparted to the atmosphere is evaluated on the basis of the above budget, i.e. as a difference between incoming net solar radiation and both sensible and latent heat fluxes, respectively. This implies that the latter have to be determined by means of suitable schemes based on specific physical quantities. Some of these schemes will be briefly recalled below.

3.1 Ground heat flux: Q_G

Ground heat flux is dominated by molecular processes which are properly modelled by the Fourier law for heat conduction. However simplified models are often conveniently adopted. In the so-called *force-restore method* (Stull 1988) the soil is assumed to be composed of two homogeneous layers: the superficial layer, affected by the daily thermal cycle, and a deeper soil layer, displaying constant temperature. The effective depth of the first layer can be estimated from the so-called *penetration depth* determined when solving the heat conduction problem. Further simplified schemes can be found in Stull (1988) along with detailed discussion of the rationale behind them. We recall only briefly two of them: ground heat flux can be roughly evaluated as a fixed fraction of the incoming net radiation flux:

$$Q_G = X\, Q_s^* \tag{2}$$

where $X = 0.1$ during daytime and $X = 0.5$ during nighttime, or also assuming it is a fraction, typically 3/10, of sensible heat flux:

$$Q_G = 0.3\, Q_s^* \tag{3}$$

3.2 Latent and sensible heat fluxes: Q_H, Q_E

The vegetation coverage plays an important role in the water exchange of an area as a source of water vapour flux into the atmosphere. Monteith (1975) and Monteith and Unsworth (1990) provided one of the most widely adopted formulations for sensible and latent heat fluxes taking into account the influence of the vegetation. Starting from previous work by Penman, he introduced a quantity, the *leaf resistance*, to reproduce, by means of a concept borrowed from hydraulics, the physiological process of water flux through leaf structure and water vapour release into the atmosphere. The Monteith equations for sensible and latent heat fluxes are:

$$Q_H = \frac{r_H s_{cc}(-Q_s^* + Q_G) + \rho C_p[q_s(z) - q(z)]}{r_H s_{cc} + \gamma(r_E + r_{ST})} \tag{4}$$

$$Q_E = \frac{\gamma(r_E + r_{ST})(-Q_s^* + Q_G) + \rho C_p[q_s(z) - q(z)]}{r_H s_{cc} + \gamma(r_E + r_{ST})} \tag{5}$$

where r_H is the aerodynamic resistance to sensible heat transfer and s_{cc} is the specific humidity variation with temperature in saturation conditions, while γ is the psychrometric constant and $q(z)$ is the air specific humidity, the subscript "s" indicates the values for saturated air.

A much simpler parameterization of the partition between sensible and latent heat fluxes at ground level assumes an overall constant value of the *Bowen ratio* coefficient:

$$\beta_R = \frac{Q_H}{Q_E} \tag{6}$$

3.3 Thermally driven slope winds

Slope winds are airflows occurring along any sloping terrain due to heating or cooling of the lowest air layers as a consequence of the diurnal cycle of incoming solar radiation and outgoing longwave radiation at night. This phenomenon is particularly evident in mountain valleys, where significant temperature gradients affect the atmospheric layers closer to mountain slopes. Heating and cooling of valley sidewalls not only produce slope flows but also more extended motions of the whole air filling the valley volume resulting in overall valley winds, i.e. airflows bringing alternatively air into or out of the valley. A detailed review of these phenomena can be found in the classical papers by Wenger (1923) and Wagner (1938) or in the more recent review by Whitenam (1990). A clear picture of the diurnal cycle of slope and valley winds has been provided in the well known sketch by Defant (1949) reproduced in Figure 3.

3.4 Theoretical formulation

A key idea to help understand thermally induced slope flows has been provided by Prandtl's (1942) work. Consider a plane surface tilted at an angle α with respect to the horizontal and unperturbed stable stratified free atmosphere far enough from the surface. It is convenient to adopt a reference frame with one axis along the slope (s coordinate) and the other axis normal to the slope (n coordinate).

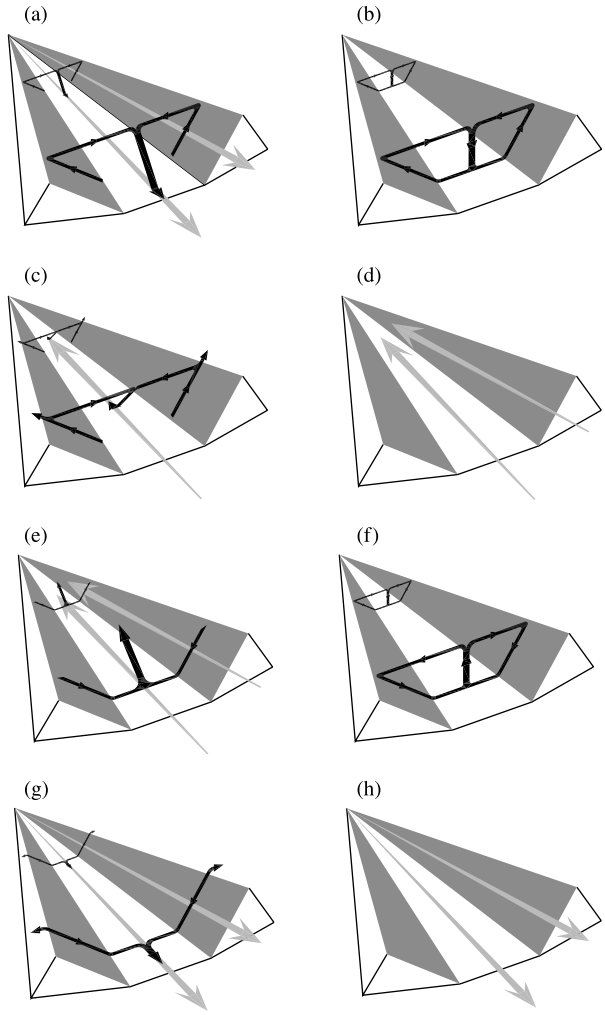

Figure 3 Diurnal cycle of valley winds. A. Sunrise: onset of up-slope winds (white arrows), continuation of mountain wind (black arrows). Valley cold, plains warm. B. Forenoon (about 09:00): strong slope winds, transition from mountain wind to valley wind. Valley temperature same as plain. C. Noon and early afternoon: diminishing slope winds, fully developed valley wind. Valley warmer than plains. D. Late afternoon: slope winds have ceased, valley wind continues. Valley is still warmer than plain. E. Evening: onset of down-slope winds, diminishing valley wind. Valley slightly warmer then plains. F. Early night: well developed down-slope winds, transition from valley wind to mountain wind. Valley and plains at same temperature. G. Middle of the night: down-slope winds continue, mountain wind fully developed. Valley colder than plains. H. Late night to morning: down-slope winds have ceased, mountain wind fills valley. Valley colder than plain (after Defant 1949)

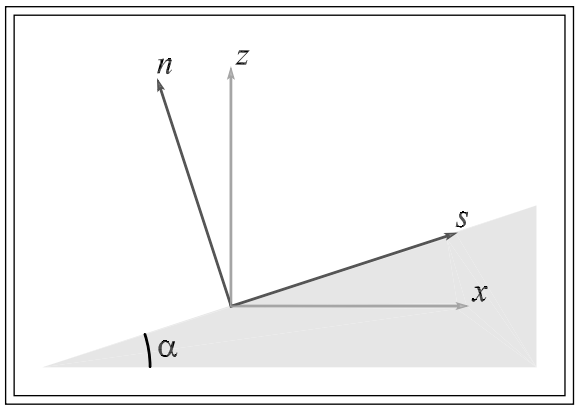

Figure 4 Reference frame used: axis *s* parallel to the slope, axis *n* normal to the slope

As widely used in meteorology, heat exchange is related to *potential temperature*, i.e. the temperature an air parcel volume would have if led to a reference pressure p_0 (typically 1,000 [hPa]), along an adiabatic transformation. Absolute temperature T and potential temperature θ are tied by a Poisson equation:

$$\theta = T\left(\frac{p_0}{p}\right)^{\frac{R_d}{c_p}} \tag{7}$$

where p is the atmospheric pressure, $R_d = 287$ [J K^{-1} kg^{-1}] is the gas constant for dry air and $c_p = 1{,}004$ [J K^{-1} kg^{-1}] is the specific heat at constant pressure (Stull 1988). Potential temperature in the unperturbed atmosphere displays a constant positive vertical gradient, while heating or cooling of the terrain surface produces a potential temperature anomaly $\Delta\theta$, so that the resulting thermal structure can be written as:

$$\theta = A + \gamma z + \Delta\theta(n) \tag{8}$$

where z is the vertical coordinate and γ is the potential temperature vertical gradient in standard atmospheric conditions. At any point on the slope the airflow velocity u is parallel to the slope and depends only on the distance above the ground, measured along the direction n perpendicular to the slope. Then wind velocity can be expressed as:

$$u = C\sqrt{\frac{g\beta\nu_H}{\gamma\nu_k}}\, e^{-n/l} \sin(n/l) \tag{9}$$

while the anomaly of potential temperature at any distance n from the surface is:

$$\Delta\theta = Ce^{-n/l}\cos(n/l) \tag{10}$$

The parameters which appear in these two equations are:

C potential temperature anomaly at ground level: $Dq(v)|_{v=0}$;
g acceleration due to gravity;
$\beta = 273.15^{-1}$;

ν_H air thermal diffusivity;
ν_k air kinematic viscosity;

$l = \sqrt[4]{\dfrac{4\nu_H\nu_k}{g\beta\gamma\sin\alpha}}$ typical length scale of the phenomenon; and

α slope angle.

The value of C, which is in fact an integration constant, can be determined by imposing a suitable boundary condition at the interface ground-atmosphere. At ground level, the conduction of sensible heat is responsible for temperature modification, which is conveniently described in terms of the Fourier law:

$$Q_H = -k_H \left.\frac{\partial \Delta\theta}{\partial n}\right|_{n=0} \tag{11}$$

where Q_H is the sensible heat flux and $\dfrac{\partial \Delta\theta}{\partial n}$ is the potential temperature variation in the n direction at ground level: the variation in the s direction does not occur as far as the motion and can be assumed to be uniform along the slope.

Substituting Equation (10), for the anomaly of potential temperature, into Equation (11) we obtain an expression for C:

$$C = \frac{Q_H l}{k_H} \tag{12}$$

The thermodynamic variable that allows us to take into account the effects of water vapour is the virtual potential temperature, since this quantity depends on the specific humidity q:

$$\theta_v = (1 + 0.61q)\,T\left(\frac{p_0}{p}\right)^{\frac{R_d}{c_p}} = \theta(1 + 0.61q) \tag{13}$$

The expression for the virtual potential anomaly $\Delta\theta_v''$ and for the velocity u can be determined as in the previous case. In the moist case boundary conditions are different to take into account evaporation processes. Profiles and isosurfaces for θ_v and u can be obtained in the same way as in the dry case, but the proper boundary condition, in addition to the heat budget (1), is the conservation of moisture flux F_w along with the given value of the Bowen ratio:

$$Q_E = F_w = C_e \frac{L_e}{c_p}\, u\Big|_{n=0}\left(q_p - q\Big|_{n=0}\right) \tag{14}$$

$$\beta_R = \frac{Q_H}{Q_E} = \frac{-\tilde{k}\left.\dfrac{\partial \theta_v''}{\partial n}\right|_{n=0}}{C_e u\Big|_{n=0}\left(q_p - q\Big|_{n=0}\right)} \tag{15}$$

where L_e is the latent heat for water. For further details see Rea (2002).

Criteria to evaluate sensible heat flux on the basis of land properties, incoming solar radiation and atmospheric conditions will be explained below.

4 Implementation

The Prandtl (1942) formulation for slope winds has been solved imposing two different sets of boundary conditions to model wind velocity, potential and virtual potential temperature. Using these quantities it is therefore possible to describe air humidity in the layers close to the slope. Essentially, the parameters the formulas depend on are: the coordinate n, the humidity flux at the surface, the sensible and latent heat fluxes at the ground level which can be described solving the energy balance. This information has to be known for every point in the 3D control volume, outlined using voxel (volume pixel), three-dimensional raster elements. Two different approaches have been developed to implement the mathematical models within the GRASS GIS (Ciolli et al. 2002a, b). New GRASS support for 3D rasters and maps algebra has been used together with classical 2D features and capability.

4.1 A full 3D approach for wind velocity and potential temperature

To implement the Prandtl solution for slope winds for every voxel in the volume the evaluation of its distance from the slope surface measured along the direction normal to the surface, is needed. Moreover, each voxel must be assigned the value of the sensible heat flux at the point on the slope surface in the normal direction defined by the current raster element. Since the volume is outlined by a 3D raster, every voxel has its own set of coordinates (row, column, level), moreover the slope surface is described by a DTM raster map. From the DTM it is possible to extract information about slope angle and aspect angle for each cell. Therefore, available geometric information is: 3D coordinates of the volume elements and of the DTM elements and local information about slope and aspect angles. By geometric considerations it is possible to obtain an analytic formulation for the coordinate n. The equation to evaluate the coordinate n can be obtained considering Figure 5, its projection on the horizontal plane and on the vertical plane containing AN.

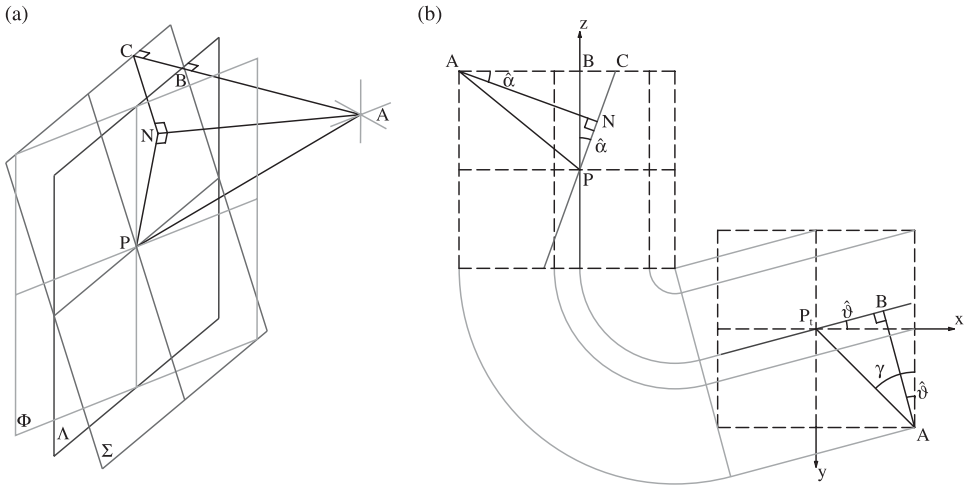

Figure 5 (a) Outline of the geometric system – terrain surface Σ and point A in the volume, and (b) Geometric

Defining the quantities:

$$\begin{aligned} \Delta x &= x_A - x_P \\ \Delta y &= y_A - y_P \\ \Delta z &= z_A - z_P \\ \hat{\alpha} &= \frac{\pi}{2} - \alpha \quad \alpha = \textit{slope angle} \\ \hat{\vartheta} &= \frac{\pi}{2} - \vartheta \quad \vartheta = \textit{aspect angle} \end{aligned} \tag{16}$$

and following simple geometric considerations the distance $\overline{AN}$ can be expressed by:

$$\overline{AN} = \left\{ \sqrt{\Delta x^2 + \Delta y^2} \cos\left[\tan^{-1}\left(\frac{\Delta x}{\Delta y} \right) - \hat{\vartheta} \right] + \Delta z \tan(\hat{\alpha}) \right\} \cos(\hat{\alpha}) \tag{17}$$

Equation (17) depends on the coordinates of the voxel and on the coordinates of the DTM cell belonging to the normal direction. This particular DTM cell can be located considering a noticeable feature elementary geometry: a segment starting from a point A and normal to a surface is the shortest segment connecting A to the surface. Once the element on the slope surface (DTM) which belongs to the normal direction has been located, it is possible to connect to every voxel the value of information related to the surface and not just the sensible heat flux at ground level.

A new 3D raster module has been developed, for the GRASS GIS, to evaluate the coordinate n in the entire 3D domain and to generate a 3D raster where each cell is assigned the value of the cell on the surface belonging to the same normal vector. In this way it is possible to transfer bi-dimensional information (2D raster map) into a 3D environment where data can be managed and analyzed using map algebra. The module **`r3.isosurf`** searches the cell of the DTM providing the shortest distance from the current voxel, applies the n coordinate formula and stores the coordinates (row, column) of the DTM cell which solves the problem. Then the module, depending on the user choice, produces the 3D raster map for the n coordinates or a 3D raster map where each voxel is assigned the value of the sensible heat flux in the closest DTM cell. Depending on the DTM geometry there are some configurations where it is not possible to define any normal direction to the ground surface. The module solves these situations in a quite simple way; three solutions have been provided. A first solution is to leave these cells empty. A second one is to apply Equation (17) with respect to the closest DTM cell. A third solution is to assign these cells the value of the shortest distance from the DTM.

The wind velocity and the potential temperature of the air above the slope also depend on the value of the sensible heat flux at the ground level. This flux is related to the ground heating and cooling, which can be described by the energy balance on the slope surface. In many equations the energy balance is a function of the solar beam's incidence angle. This angle is defined as the angle between the solar beam's vector and the direction normal to the surface. Using the GRASS module **`r.sun`** it is possible to obtain such information for every cell describing the slope surface. Knowing the solar incidence angle it is possible to use many different parameterizations to describe each term of the heat exchanges at the surface level. Using the GRASS support for map algebra it is possible to implement formulations which take into account atmospheric parameters such as absorption, reflection and transmission coefficients, atmospheric

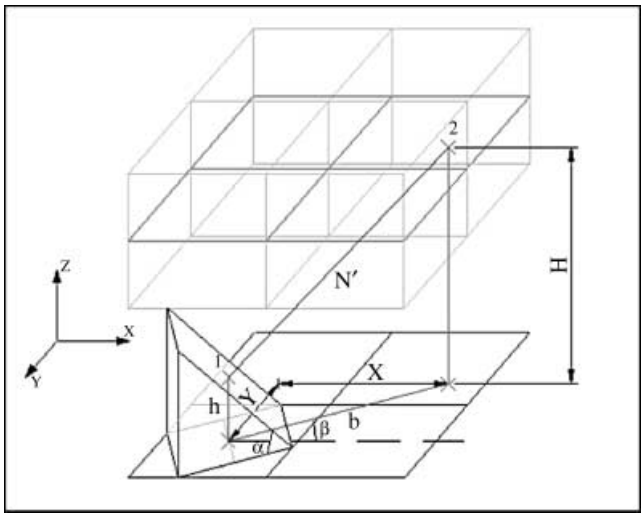

Figure 6 Reference frame used: axis *s* parallel to the slope, axis *n* normal to the slope

transmissivity and a cloud cover factor. In addition, vegetation cover related information such as leaf resistance to water vapour flux, albedo and soil thermal capacity can be considered.

Once the sensible heat flux 2D raster map is available, the new module can be used to produce the 3D map of the coordinate *n* and to transfer sensible heat flux values to a second 3D map. Using the GRASS support for the three-dimensional map algebra these maps have been combined to implement Equations (8) and (9) to produce one 3D map for the potential temperature and one for the wind velocity. A more detailed description of the procedure can be found in Vitti (2002).

4.2 A 2½D approach for humidity flux and virtual potential temperature

Another approach can be followed to evaluate the coordinate *n* and to transfer bi-dimensional maps into 3D maps. Since the 3D raster maps can be thought of as a series of 2D maps stacked one over the other, the idea is to create a 3D raster by laying a copy of the same 2D map one over the other. In this way it is possible to use the 3D map algebra to manage 2D information. The coordinate *n* is also evaluated by this "layers" approach using only the 3D map algebra. Starting from the bottom level and going upward the implemented formula searches the DTM cell whose normal vector passes through the current voxel and then evaluates a first approximated value of this vector. Geometric adjustments are necessary to obtain the correct value of the vector module. Figure 6 outlines the geometry configuration that serves as the basis for this approach.

The value N' of the normal segment can be evaluated as:

$$N' = b\cos(\omega - \beta)\sin\alpha + (H - h)\cos\alpha \tag{18}$$

where α = slope angle, β = aspect angle, b = horizontal distance between point 1 and 2, ω = angle between b and x direction, H = height of the current level and h = height of the current DTM cell.

The 3D cells which are not passed by any normal direction from the slope surface are, in a first step, left empty. Once all the levels have been processed the empty cells are assigned the mean value of the surrounding cells, in this way a solution is provided, however some artificial smoothing is introduced. The number of cells which has to be considered to extract the mean value can be specified by the user.

This second approach leads to the evaluation of the virtual potential temperature and humidity flux in the atmospheric layers close to the slope surface. The wind velocity has to be evaluated in every voxel and the energy balance at ground level has again to be solved to produce the sensible and latent heat flux 2D maps. Once this information is available the 2D maps are used to generate the respective 3D maps to be managed by 3D map algebra. The integration constants are also evaluated at this step to obtain local values of virtual potential temperature and humidity flux.

The energy balance is solved using the "Bowen ratio" parameterization, which describes the ratio between sensible and latent heat flux. For a given day, the daily mean value of the incoming solar radiation is produced by the GRASS module **`r.sun`** which integrates the relevant irradiance between sunrise and sunset times. Through opportune expressions which take into account the position of the sun in the sky and the interaction of the solar radiation with the atmosphere (Iqbal 1983) the value of the solar irradiance for a shorter time period can be obtained.

5 Test and Applications

The two developed methods describe different atmospheric quantities such as potential and virtual potential temperature, humidity flux and wind velocity, considering both a dry and moist atmosphere. Different equations have been applied and implemented using the GRASS support for 3D map algebra; moreover, two different approaches have been implemented within GRASS to accomplish the atmospheric modeling.

Some tests were made before applying the models to a real domain. As a first step, the new developed GRASS module was tested. Then four applications were realized by gradually increasing the complexity of the physical domain, such as the geometry of the slope and its features, and removing simplifying hypotheses on the atmospheric model, such as considering a moist atmosphere. The applications scheme is summarised in Figure 7.

5.1 Module test

A set of synthetic DTMs was generated to verify the quality of the results provided by the new GRASS module. A first slanted plane was used mainly to verify Equation (17) that evaluates the coordinate n. Another test was executed using a more complex DTM built to have a large number of cells for which a normal direction does not exist. Good results can be obtained also in the zones where the normal direction cannot correctly or univocally be defined. The isosurfaces shown in Figure 8 are obtained using the GRASS 5 visualization module, the data are really 3D and not 2D data "spread" over a DTM.

5.2 Prandtl simple formulation, ideal slope and moist air

The first application tests the model to verify the consistency with the 2D control measurement collected by Defant (1949). In his research Defant measured wind slope

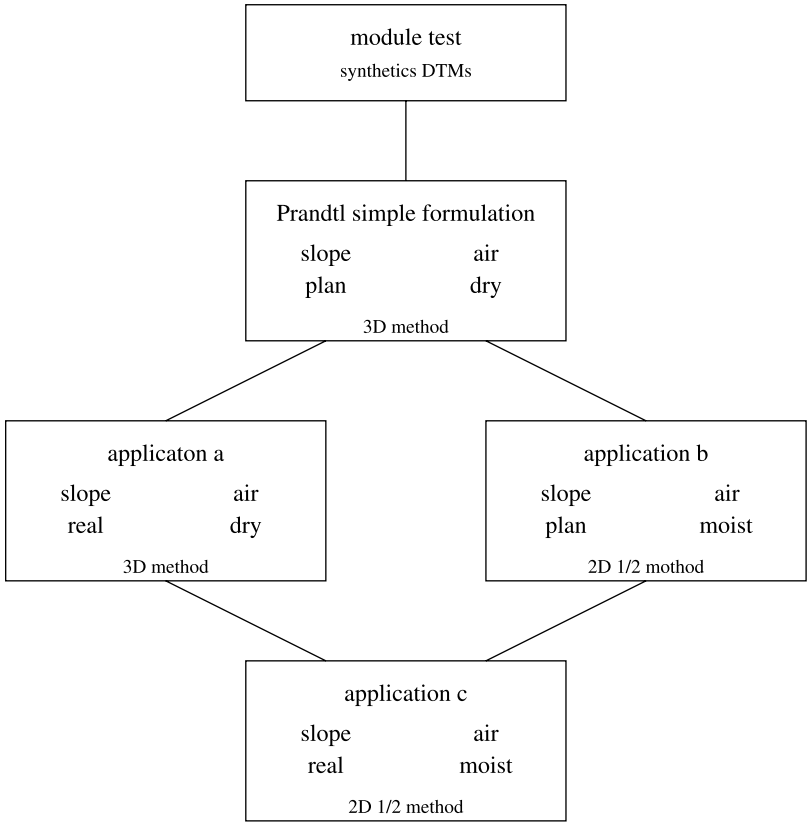

Figure 7 Scheme of the executed applications

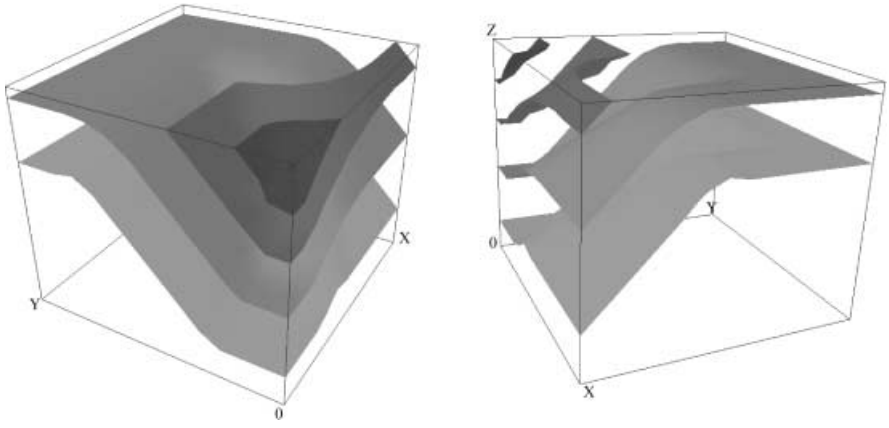

Figure 8 GRASS 5 visualizations of surfaces with constant distance from a synthetic DTM

Table 1 Defant experimental parameters

Parameters	Value	
α	42.5	[°]
C	3.4	[°C] upslope
A	22.25	[°C]
λ	34.37	[m]
γ	0.004	[°C m^{-1}]
$C\sqrt{\frac{g\beta\nu_H}{\gamma\nu_k}}$	11.82	[m s^{-1}]

velocity in a location near to Innsbruck, Austria along a uniform valley side, with constant aspect and slope angles, constant vegetation cover and stable atmosphere in good meteorological conditions. For the test, a slanted plane DTM, similar to Defant's measurement site, was used and since the atmosphere was considered to be moist, no humidity flux was therefore taken into account. The parameters used to solve Equation (9) for the wind velocity are shown in Table 1. The DTM planimetric resolution is 100×100 [m] and the vertical resolution of the 3D output raster map is 100 [m] (Plate 13).

5.3 Application to a real slope and dry air

The model was next applied to a site on the eastern side of the Adige valley south of the city of Trento (Italy) in the Alps. The model has been applied on a 10×10 [m] DTM, supplied by the *Provincia Autonoma di Trento*, to obtain the 3D raster map of the coordinates n. In particular two smaller areas, using a $10 \times 10 \times 10$ [m] resolution, were studied. The value of the potential temperature anomaly at ground level, was obtained from Equation (10):

$$\Delta\theta = Ce^{-n/l}\cos(n/l) \tag{19}$$

The parameter λ/k_H was estimated assuming a sensible heat flux of 150 [W m^{-2}] producing a potential temperature anomaly C of 3.4 [°C]. In Defant's (1949) work, a value of 3.4 [°C] for C was computed by integrating experimental observations and mean conditions of a slope in the early morning hours. A value of 150 [W m^{-2}] is a reasonable estimate for sensible heat flux in the late morning (Stull 1988).

The steps used to apply the model inside GRASS are as follows. Module **`r.sun`** gives the solar incidence angle θ_n for a given day and hour. The downward radiation flux K_s is calculated using:

$$K_s\downarrow = SE_0T_k\cos\theta_n \tag{20}$$

where $E_0 = 0.997$ is the orbital coefficient and the atmosphere has been assumed absolutely clear so that atmospheric transmissivity coefficient is simply: $T_k = 0.6 + 0.2\cos\theta_n$ (Iqbal 1983). Reflected radiation flux is evaluated adopting a value of 0.14 for the albedo coefficient a of a vegetation cover (Iqbal 1983). The long wave radiation flux was set to $I^* = 93.4$ [W m^{-2}] (Stull 1988). The above equations were implemented in

GRASS using **r.mapcalc** to obtain a set of 2D raster maps that were combined together to produce the potential temperature anomaly 2D map. This raster map became the input for the module **r3.isosurf**. Finally all the model input parameters are available as 3D maps, in particular all the variables of Equation (9). Therefore it is possible to use the 3D map algebra to obtain the 3D map of the slope wind velocity (Plate 14).

5.4 Application to an ideal slope and moist air

The model was also applied to some simple cases in order to evaluate the sensitivity to the variation of some parameters. The overall conditions are stationary and related to the structure of up-slope winds. The first application was on an ideal slope with constant inclination, aspect, vegetation and physical characteristics. The values of Q_s, C_e and q_p are constant in every cell. In addition, L_e, ν, c_p, k_h and k_v were regarded as constant. Different values of the parameters C_e and q_p were set in a range in order to evaluate model's sensitivity to their variation. The parameters that were changed are:

- C_e water vapor bulk transfer coefficient
- q_p specific humidity of vegetation surface
- γ linear coefficient of undisturbed θ_v profile
- λ characteristic length
- α slope inclination
- Q_s solar radiation

The mean values of the parameters are reported in Table 2. The analysis has been performed observing profiles along the normal direction and sections of the isosurfaces visualized in VIS5D. The virtual potential temperature profile and the section of the isosurfaces for mean values of the parameters are similar to those obtained by Defant (1949) for potential temperature, but these results are related to virtual potential temperature and to moist air. The values of virtual potential temperature are in a range of about 290–305 [K] but these values depend also on the imposed value of undisturbed θ_v near the soil.

Table 2 Mean values of the parameters in ideal valley applications

Parameters	Value	
q_p	0.012	$[g_{water}:g^{-1}]$
C_e	0.02	[–]
γ_q	-1.937×10^{-6}	$[m^{-1}]$
γ	2.68×10^{-3}	$[K:m^{-1}]$
λ	35	[m]
D	0.00807	$[g_{water}:g^{-1}]$
A	294	[K]
c_p	1005	$[J:kg^{-1}:K^{-1}]$
L_e	2.5×10^{-6}	$[J:kg^{-1}]$
ρ	1.293	$[kg:m^{-1}]$

First, the sensitivity to q_p and C_e was tested since increasing these two parameters has the same effects:

- on the profiles, it produces an increment of θ_v near the surface;
- on the isosurfaces, it causes the growth of the "mixing" zone near the ground surface.

Variation of characteristic length λ acts directly on the thickness of the layer in which the virtual potential temperature anomaly $\Delta\theta_v''$ has effect: the increasing of λ increases the thickness. So the effects of the virtual potential temperature anomaly are amplified when the thickness of the layer decreases. Effects of slope inclination α and solar radiation Q_s act in the opposite direction: the decreasing of α increases the value of θ_v near the ground surface, the increasing of Q_s has the same effect. The relationship of the linear coefficient of the undisturbed θ_v profile, γ, with the virtual potential temperature profiles causes an increase in θ_v near the soil and a decrease over 50–100 [m], when γ increases; increasing γ also increases the modulus of θ_v isosurfaces.

The velocity profiles are comparable with those in the literature and the values are similar to the results of Defant (1949), even if values of velocity are sometimes smaller, about 1–3 [m s^{-1}]. The biggest difference with usual profiles is that velocity is not equal to zero for $n = 0$ (i.e. at the top of vegetated layer) where the humidity flux and energy balances are imposed. In this case the *slip velocity* appears on the canopy surface and this is an important peculiarity of this solution. The increasing of q_p and C_e decreases the values of u near $n = 0$ and increases its values for $n > 30$ [m]; the decreasing of these two parameters has the opposite effect. This fact is correlated to the equipotential surfaces of θ_v and the thickness of the "mixing" zone: F_w is imposed by setting the value of the Bowen ratio and velocity must change to satisfy the energy and humidity balances. Positive variations of λ decrease the values of u and increase the thickness of the layer in which $\Delta\theta_v''$ has effect. The increasing of Q_s and decreasing of α increases the value of u along the profile, but Q_s increases *slip velocity* too, while α has no effect on it. On the other side increasing γ causes the decreasing velocity modulus.

5.5 Application to a real slope and moist air

This trial application was performed in order to evaluate the effect of DTM morphology and complex geometric configuration on the model results, particularly on the shape of virtual potential temperature isosurfaces. Terrain morphology was obtained from Trento Province DTM's with a resolution of 40 [m]. Solar radiation was obtained with the **`r.sun`** module. The other parameters were assumed constant and their mean values are reproduced in Table 2. In this case the simulation was performed only on sections of θ_v equipotential surfaces because the sensitivity analysis of profiles and velocity would bring the same results as those obtained for an ideal valley. Until the slope is regular the solution is similar to the case of the ideal valley, otherwise some variations can be seen: when the slope softens the isosurfaces are closed; in this zone the slope inclination is small and the solar radiation is large so the two effects that increase $\Delta\theta_v''$ add, therefore θ_v increases rapidly. The variation of the other parameters has the same effect as in the previous application:

- q_p and C_e act on the thickness of the mixed layer;
- λ influences the zone in which θ_v'' has effect; and
- increasing γ increases the values of $\Delta\theta_v$ (Figure 10).

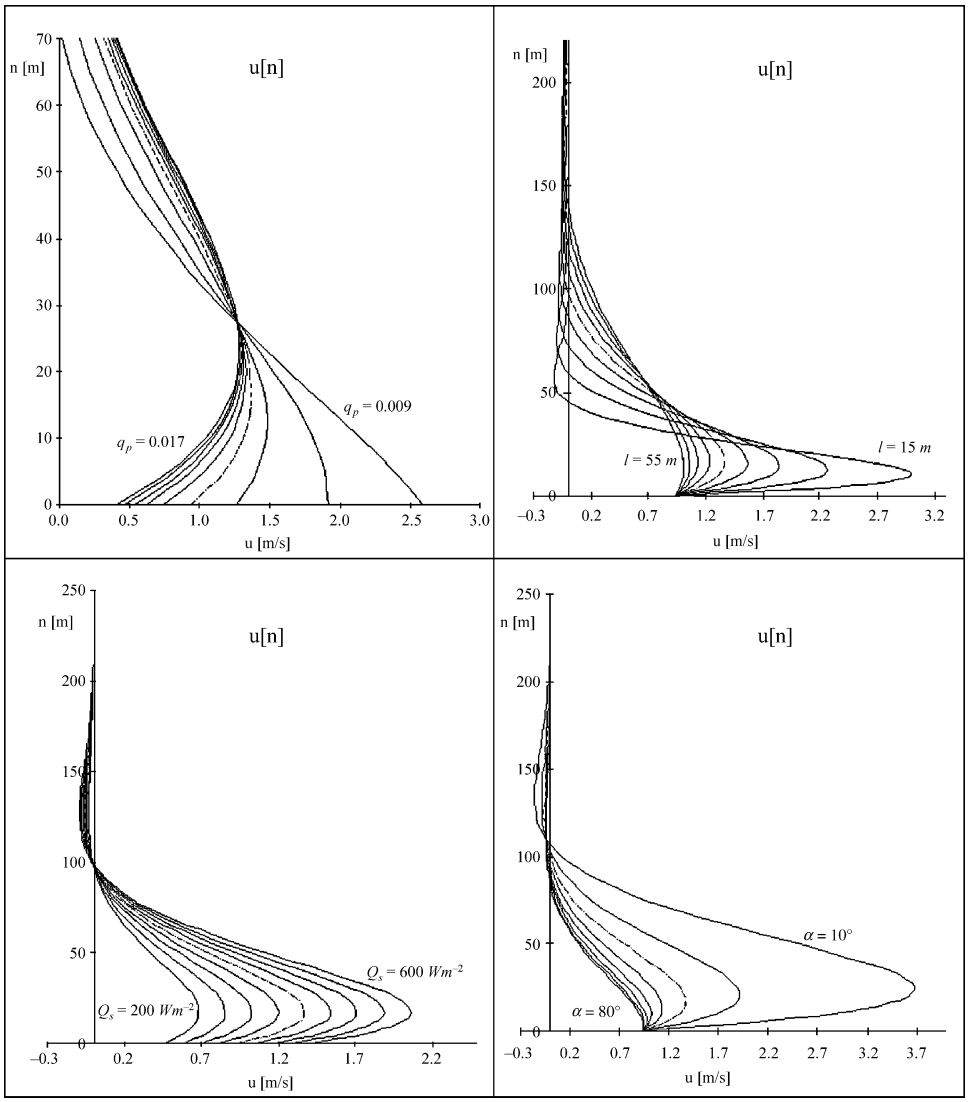

Figure 9 Effects on velocity profile due to q_p, λ, Q_s and α variations; dotted line indicates the profile for mean value of the parameters

6 Conclusions

An application exploiting the capabilities of GRASS 5 for managing and analyzing landscape information and geographic data by means of integrated and complementary use of both the 2D and 3D GRASS modules has been proposed. The application facilitates the simulation of atmospheric phenomena closely dependent on ground and landscape features, such as the local heat budget at the ground surface and the development of thermally induced slope winds. Based on the classical solution for up- and down-slope wind

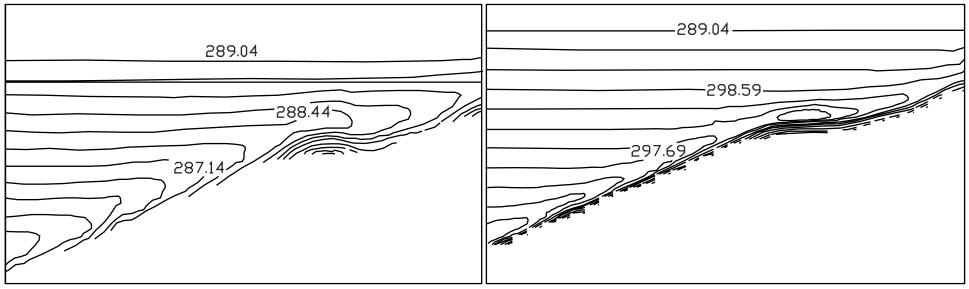

Figure 10 Variation of the v isosurfaces by changing the value of λ. Left for $\lambda = 50$ [m] and right for $\lambda = 25$ [m]

generation provided by Prandtl (1942), an estimate for wind strength and temperature anomaly of air layers close to the ground at each location in the domain was evaluated. As the solution depends on the coordinate n locally normal to the surface at each point, a suitable procedure to obtain 3D maps of the modulus of the normal to the slope was implemented in 3D algebra. Calculated values are based on estimation of local values of physical parameters and evaluation of the local heat budget using information on solar radiation from **`r.sun`** and vegetable cover. Further extension of Prandtl's (1942) solution was provided in order to take into account moist air and evaporation processes in terms of virtual potential temperature associated to specific humidity. Boundary conditions are slightly different and energy and humidity flux balances were imposed on the contact surface between atmosphere and vegetation, where a suitable "slip velocity" was assumed. Equations for moist air solution were implemented in **`r3.mapcalc`** and boundary conditions were calculated using 2D modules like **`r.sun`**, **`r.mapcalc`** and **`r.slope.aspect`**. The results obtained display good qualitative agreement with typical patterns shown by field measurements (Whiteman 1990, Rampanelli and Zardi 2003) and modeling (Rampanelli et al. 2003). Further comparison on a quantitative basis is among possible further developments in connection with ongoing research projects.

The sensitivity of the solution to the variation of some parameters was also evaluated. Future possible developments include the implementation of more complex parameterization to improve the actual case analysis. A remarkable improvement in the **`r3.isosurf`** module would involve splitting it into two modules: one to produce the 3D maps of the n coordinates which are related to the no-time dependent DTM geometry and another to produce, from existing 2D, as many 3D maps as the user needs. Other possible applications could be mapping quantities related to other phenomena, such as concentration of pollutants and parameters for estimation of landslide and avalanche phenomena.

References

Ciolli M, Vitti A, Zardi D, and Zatelli P 2002a 2D/3D GRASS modules use and development for atmospheric modelling. In Benciolini B, Ciolli M, and Zatelli P (eds) *Proceedings of Open Source Free Software GIS – GRASS Users Conference*, University of Trento, Italy

Ciolli M, Rea R, Zardi D, and Zatelli P 2002b Modelling of evaporation processes over tilted slopes by means of 3D GRASS raster. In Benciolini B, Ciolli M, and Zatelli P (eds)

Proceedings of Open Source Free Software GIS – GRASS Users Conference, University of Trento, Italy

Defant F 1949 Zur theorie der Hangwinde, nebst Bemerkungen zur Theorie der Berg- und Talwinde *Archiv fuer Meteorologie Geophysik und Bioklimatologie* Ser. A, 1: 421–50

Iqbal M 1983 *An Introduction to Solar Radiation*. New York, Academic Press

Monteith J L 1975 *Vegetation and the Atmosphere*. New York, Academic Press

Monteith J L and Unsworth M H 1990 *Principles of Environmental Physics*. London, Edward Arnold

Neteler M and Mitasova H 2002 *Open Source GIS: A GRASS GIS Approach*. Boston, MA, Kluwer

Prandtl L 1942 *Führer durch die Strömungslehre*. Braunschweigh, Vieweg und Sohn

Rampanelli G and Zardi D 2002 Identification of thermal structure from airborne measurements in an Alpine valley with Kriging technique. In *Proceedings of the Tenth AMS Conference on Mountain Meteorology*, Park City, Utah: 93–6

Rampanelli G, Zardi D, and Rotunno R 2003 Mechanisms of up-valley winds. *Journal of Atmospheric Sciences* (submitted)

Rea R 2002 Study of Evaporation Processes over a Slope by Means of Three-dimensional Modelling in GIS GRASS. Unpublished Ph.D. Dissertation, School of Environmental and Land Planning Engineering, University of Trento

Stull R B 1988 *An Introduction to Boundary Layer Meteorology*. Boston, MA, Kluwer

Vitti A 2002 Three-dimensional Modelling Using the GRASS GIS of Thermally Driven Slope Winds. Unpublished Ph.D. Dissertation, School of Environmental and Land Planning Engineering, University of Trento

Wagner A 1938 Theory and observation of periodic mountain winds. *Gerlands Beitr Geophysik* 52: 408–49

Wenger R 1923 Zur theorie der berg- und talwinde. *Meteorologische Zeitschrift* 40: 193–204

Whiteman C D 1990 Observation of thermally developed wind systems in mountain terrain. In Blumen W (ed) *Atmospheric Processes over Complex Terrain*. Washington, D.C., American Meteorology Society Monograph No. 23: 5–42